The ^{68m}Cu/^{68}Cu isotope as a new probe for hyperfine studies: The nuclear moments

2016 EPL 115 62002

(http://iopscience.iop.org/0295-5075/115/6/62002)

A Letters Journal Exploring the Frontiers of Physics

September 2016

EPL, **115** (2016) 62002 www.epljournal.org
doi: 10.1209/0295-5075/115/62002

The ^{68m}Cu/^{68}Cu isotope as a new probe for hyperfine studies: The nuclear moments

A. S. Fenta[1,2,3], S. Pallada[3,4,5], J. G. Correia[3,6], M. Stachura[3,7], K. Johnston[3], A. Gottberg[3,7], A. Mokhles Gerami[8], J. Röder[3,9], H. Grawe[10], B. A. Brown[11], U. Köster[12], T. M. Mendonça[3], J. P. Ramos[3,13], B. A. Marsh[3], T. Day Goodacre[3,14], V. S. Amaral[1], L. M. C. Pereira[2], M. J. G. Borge[3] and H. Haas[1,3]

[1] *Department of Physics and CICECO, University of Aveiro - 3810-193 Aveiro, Portugal*
[2] *KU Leuven, Instituut voor Kern- en Stralingsfysica - Celestijnenlaan 200 D, 3001 Leuven, Belgium*
[3] *CERN, 1211 Geneva 23, Switzerland*
[4] *Department of Chemistry, Faculty of Science, University of Copenhagen - Universitetsparken 5, 2100 Copenhagen, Denmark*
[5] *Department of Medicine, Democritus University of Thrace, Alexandroupoli Campus 6 km Alexandroupolis-Makris, 68100 Alexandroupoli, Greece*
[6] *Centro de Ciências e Tecnologias Nucleares (C2TN), Instituto Superior Técnico, Universidade de Lisboa 2686-953 Sacavém, Portugal*
[7] *TRIUMF - 4004 Wesbrook Mall Vancouver, BC V6T 2A3, Canada*
[8] *Department of Physics, K.N.Toosi University of Technology - P.O.Box 15875-4416, Tehran, Iran*
[9] *Institute of Physical Chemistry, RWTH-Aachen - Aachen, Germany*
[10] *GSI Helmholtzzentrum für Schwerionenforschung GmbH - D-64291 Darmstadt, Germany*
[11] *National Superconducting Cyclotron Laboratory and Department of Physics and Astronomy, Michigan State University - East Lansing, MI 48824-1321, USA*
[12] *Institut Laue-Langevin - 71 avenue des Martyrs, F-38042 Grenoble, France*
[13] *Laboratory of Powder Technology, École Polytechnique Fédérale de Lausanne (EPFL) - CH-1015, Switzerland*
[14] *School of Physics and Astronomy, The University of Manchester - Manchester, M13 9PL, UK*

received 24 June 2016; accepted in final form 6 October 2016
published online 7 November 2016

PACS 21.10.Ky – Electromagnetic moments
PACS 23.20.En – Angular distribution and correlation measurements
PACS 21.60.Cs – Shell model

Abstract – Time Differential Perturbed Angular Correlation of γ-rays (TDPAC) experiments were performed for the first time in the decay of ^{68m}Cu ($6^-, 721\,\text{keV}, 3.75\,\text{min}$) produced at the ISOLDE facility at CERN. Due to the short half-life of the source isotope, the measurements were carried out online. The intermediate state ($2^+, 84.1\,\text{keV}, 7.84\,\text{ns}$) offers the unique opportunity to study the electromagnetic fields acting at a copper probe in condensed matter via hyperfine interactions. The present work allowed determination of the nuclear moments for this state. The electric quadrupole moment $|Q(2^+, 84.1\,\text{keV})| = 0.110(3)$ b was obtained from an experiment performed in Cu_2O and the magnetic dipole moment $|\mu| = 2.857(6)\,\mu_N$ from measurements in cobalt and nickel foils. The results are discussed in the framework of shell model calculations and the additivity rule for nuclear moments with respect to the robustness of the $N = 40$ sub-shell.

Introduction. – Copper (Cu) in its native form is, reportedly, the first metal to be used by mankind, with mechanical, chemical and electronic properties that makes it, still today, a reference in human activities and welfare. Furthermore, Cu plays a key role in every life form [1] acting as a cofactor in metabolic enzymes, which are involved in cellular reparation, respiration or photosynthesis [2,3]. In living systems Cu is present in two oxidation states, Cu(I) and Cu(II), ruling electron transfer in vital redox mechanisms. Due to its unpaired electron

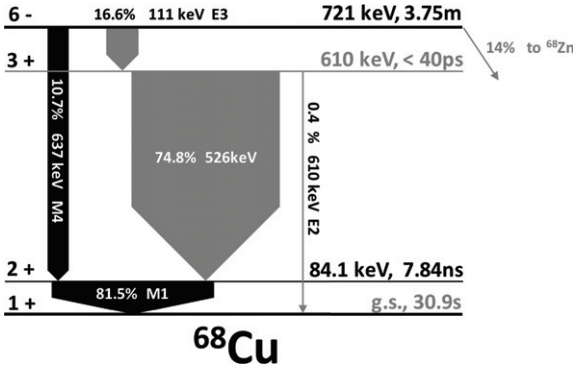

Fig. 1: Decay scheme of ^{68m}Cu/^{68}Cu. In black are the relevant gamma lines for the TDPAC experiment. Width and length of the arrows are proportional to intensity and energy, respectively.

and characteristic *d*-*d* transition absorption, Cu(II) is well studied with different spectroscopic methods [4], while Cu(I) is difficult to observe because of its closed shell (d^{10}) electronic structure leading to basically featureless spectroscopic properties. On the other hand, as a diamagnetic ion, Cu(I) can potentially be investigated by Nuclear Magnetic Resonance (NMR)/Nuclear Quadrupole Resonance (NQR) spectroscopy.

^{63}Cu and ^{65}Cu are stable isotopes which have been used very successfully in studies of bulk matter, notably recently the high-T_c superconductors. Such experiments, however, require a large amount of sample material and are often restricted to low temperatures. In biological systems, the use of the solution-phase NMR is often the method of choice for studying structure and dynamics at the metal binding sites. This technique has a very limited application to Cu(I) containing complexes, due to the large nuclear quadrupole moments of ^{63}Cu and ^{65}Cu NMR nuclei and their low gyromagnetic ratios. These cause low sensitivity and broad resonance lines [5–7]. Therefore, there is considerable interest in searching for other techniques, which have potential for characterizing the Cu(I) binding structure and electronic states in diluted concentrations of the probing isotope in biological and solid-state materials. A practical solution can be given by radioactive hyperfine techniques, such as Mössbauer spectroscopy (MS) or Time-Differential Perturbed Angular Correlation (TDPAC) [8–10]. These are sensitive to the interaction of the nuclear electric quadrupole and/or magnetic dipole moments with the electric field gradients (EFG) or the magnetic hyperfine fields (B_{hf}) generated by the external charge distribution and polarization of the host material [11]. Unfortunately, no copper isotope is available for MS experiments. By looking at the decay schemes of Cu isotopes, one finds that ^{68m}Cu with a half-life of 3.75 minutes and its decay cascade (shown in fig. 1) appears as the best TDPAC candidate to be used as a copper probe for future applications in the fields of materials physics, chemistry and biophysics. The selection of the ^{68m}Cu/^{68}Cu isomeric decay was made considering several favorable properties: a) a cascade with suitable gamma-ray energies 637 keV and 84 keV; b) an intermediate 2^+ state with 7.84 ns half-life c) a high expected angular anisotropy factor of 15%. The latter is easily measurable and defines the maximum observable amplitude of the TDPAC perturbation function. Moreover, a TDPAC cascade with a starting isomeric parent state is particularly useful, since perturbations due the electronic rearrangement following a chemical valence change after electron capture or beta decay are avoided.

The half-life of 3.75 minutes is short, but it can still allow post-implantation sample conditioning and data taking. The hyperfine interactions are measured consequently at the intermediate state (2^+, 84.1 keV, 7.84 ns). Last but not least, the current ^{68m}Cu yields available at the ISOLDE facility [12,13], when combined with an efficient detection system with good energy and time resolution, made these experiments possible.

Herein, we report the first TDPAC experiment performed on a Cu isotope, which simultaneously provided the first measurement of the nuclear electric quadrupole and magnetic dipole moments of the (2^+, 84.1 keV, 7.84 ns) state of ^{68}Cu, obtained in the isomeric decay of ^{68m}Cu. From the nuclear physics point of view these data are of particular interest, because in the empirical shell model the 1^+ ground state (*g.s.*) and the 2^+ isomer in ^{68}Cu are assumed to form a $\pi p_{3/2} \times \nu p_{1/2}^{-1}$ doublet relative to $Z = 28$, $N = 40$ ^{68}Ni. Nuclear moments are known for the g.s. and the ^{68m}Cu, 6^- isomer [14]. The present values for the 2^+ isomer doublet partner complete this information on the robustness of the $N = 40$ sub-shell closure.

Experiment. – The ^{68m}Cu$^+$ ion beam was produced online at ISOLDE by the bombardment of a UC$_x$ target with the 1.4 GeV proton beam from the CERN Proton Synchrotron Booster and selective Cu ionization using the RILIS (Resonance Ionization Laser Ion Source) [15,16]. The target/ion source parameters were optimized to enhance ^{68m}Cu/^{68}Cu and suppress surface ionized ^{68}Ga such that [Cu]/[Ga] $\approx$ 80. The pure ^{68}Cu beam with 30 keV energy was then redirected to the VITO (Versatile Ion-polarized Techniques Online) [17] beam line where a sample holder was mounted inside a quartz finger collection chamber with 2 mm wall thickness. This minimized the gamma absorption and allowed direct view to the sample. The TDPAC set-up mounted online consisted of four $LaBr_3$ gamma detectors with good energy resolution (11.6% at 84.1 keV and 3.0% at 637 keV) and time resolution of 800 ps for the selected cascade. Data acquisition was performed with the digital and FPGA signal processing DIGIPAC setup [18–20]. The detectors were positioned in a plane perpendicular to the direction of the radioactive beam, each detector placed at $\pm 90°$ and $180°$ with respect to the others, as shown in fig. 2. The samples were placed in the geometrical center of the setup. Implantation and measurement were performed simultaneously

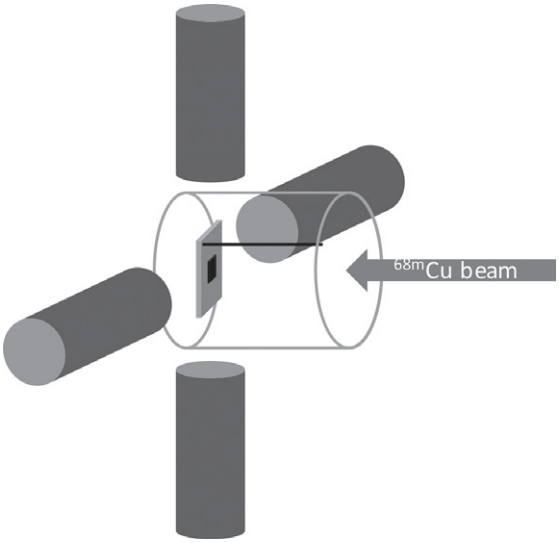

Fig. 2: Scheme of the experimental PAC set-up online at ISOLDE. The quartz finger (transparent cylinder in the center) and the four cylindrical $LaBr_3$ detectors (38 mm diameter, 38 mm length) surrounding it are shown.

at room temperature. The maximum beam intensity delivered at the sample position for ^{68}Cu in isomeric and ground state was 5×10^7 atoms/s. However, an effective lower beam intensity of about 1×10^7 atoms/s was maintained to avoid gamma pile-up saturation of the detectors, keeping a reasonable 50 kHz count rate per detector. Depending on the sample and beam conditions the data were acquired from two to four hours per sample, achieving a maximum of $2{\times}10^{11}$ implanted atoms, with an estimated dose not greater than 10^{12} at/cm^2 per sample.

Analysis. – For nuclei implanted into a polycrystalline host material, the angular probability distribution, $W(\theta)$, of finding γ_1-γ_2 emitted with a certain angle θ can be expanded into a Legendre polynomial series $P_k(\cos\theta)$ as [9,10]

$$W(\theta) = \sum_k A_{kk}\left(\gamma_1, \gamma_2\right) G_{kk}\left(t\right) P_k\left(\cos\left(\theta\right)\right); \qquad (1)$$

A_{kk} are the anisotropy coefficients of the γ-γ cascade. $G_{kk}(t)$ is the perturbation factor that contains all the information about the magnetic dipole and/or the electric quadrupole interactions. The TDPAC setup measures the number of γ_1-γ_2 coincidences, $N_{ij}(\theta, t)$, as a function of time t between detection of γ_1 and γ_2 for every pair of detectors (i, j). Then, the random coincidences are subtracted and the multiple spectra are combined correcting for efficiencies and sample misalignment in two single spectra $N(180°, t)$ and $N(90°, t)$. These are used to build the experimental perturbation function, $R(t)$, eliminating the exponential part of $N(\theta, t)$ and revealing the perturbation function to be analyzed [9,10]:

$$R\left(t\right) = 2\frac{N\left(180°, t\right) - N\left(90°, t\right)}{N\left(180°, t\right) + 2N\left(90°, t\right)}. \qquad (2)$$

For the geometry chosen here $R(t)$ is simply a sum of cosine functions of the quadrupole or magnetic interaction frequencies. Our analysis used the previously known electric field gradients and magnetic fields for copper in the selected materials, in order to extract the nuclear electric quadrupole moment, Q, as well as the nuclear magnetic dipole moment, μ, of the 2^+ state in ^{68}Cu.

In the case of integer spin I and axial symmetry of the EFG, $\eta = 0$, the quadrupole coupling constant, ν_Q, is directly related to the quadrupole moment, Q, and to the observable frequency, ω_0, by the expression

$$\nu_Q = \frac{eQV_{zz}}{h} = \omega_0 \frac{2I\left(2I-1\right)}{3\pi}, \qquad (3)$$

where V_{zz} is the principal component of the EFG tensor at the nuclear site [9,10].

In a similar way, the magnetic dipole moment can be obtained from the precession frequency, ω_L, of the magnetic moment in the magnetic hyperfine field, B_{hf}, as given by the Larmor equation:

$$\omega_L = \mu B_{hf}/I\hbar = g\mu_N B_{hf}/\hbar, \qquad (4)$$

where μ is the magnetic dipole moment of the intermediate state of the probe nuclei and g the dimensionless g-factor.

The analysis of the observable perturbation function, $R(t)$, depends on several factors such as the time resolution of the experimental apparatus and the probing state lifetime that determines the observable frequencies, the latter being proportional to the product of the hyperfine fields and nuclear moments.

Results. – Figure 3 illustrates the $R(t)$ experimental perturbation functions obtained for 3a) ^{68}Cu in Cu_2O, 3b) ^{68}Cu in Co and 3c) ^{68}Cu in Ni. All the fits to the experimental data were performed assuming a solid angle corrected, effective anisotropy coefficient $A_{22}^{eff} = -0.13(1)$ for the angular correlation of the γ_1(637 keV)-γ_2(84 keV) cascade with theoretical values expected for this cascade $A_{22} = -0.1545$ and $A_{44} = 0$ [21,22]. For the data fitting procedure, we refer the readers to [23,24] and references therein. When there is evidence for multiple sets of nuclei interacting with different local environments the fit function considers a summation of $G_i(t)$, describing each perturbation factor, weighted by the respective fraction of nuclei, f_i, where $\sum f_i = 1$.

Copper oxide, Cu_2O, known as cuprite, was chosen to measure the nuclear quadrupole interaction and determine the quadrupole moment, Q, of the ^{68}Cu, 2^+ excited state. Cuprite has a simple cubic structure, in which oxygen is tetrahedrally coordinated by copper atoms, while copper is linearly coordinated by two oxygen atoms. Due to this low coordination of Cu, this site has a non-cubic point symmetry and a strong EFG with zero asymmetry parameter, $\eta = 0$. The fitting of the experimental perturbation function $R(t)$ (fig. 3(a)) shows a predominant fraction of 89(3)% of ^{68}Cu with a characteristic quadrupole frequency $\omega_0 = 21.3(3)$ Mrad/s and $\eta = 0$. For spin 2, the respective

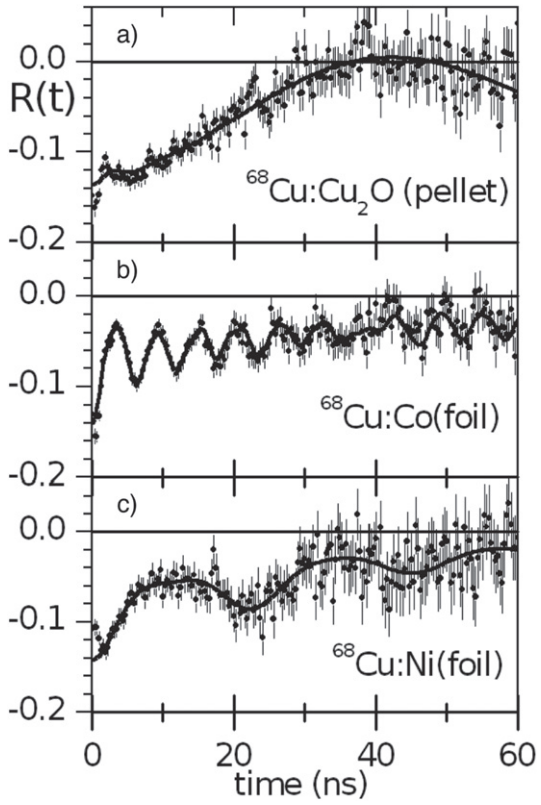

Fig. 3: The $R(t)$ function obtained from the decay of ^{68m}Cu implanted in different host materials: a) Cu_2O (pellet), b) Co (foil), c) Ni (foil).

quadrupole coupling constant is $\nu_Q = 27.14(44)$ MHz. Knowing ν_Q and using the quadrupole coupling constant $\nu_Q(^{65}\mathrm{Cu}, \mathrm{g.s.}, 3/2) = 48.138(12)$ MHz for ^{65}Cu nuclei in Cu_2O obtained by nuclear quadrupole resonance (NQR) measurements [25] the ratio of the quadrupole coupling constants is obtained. With the quadrupole moment $Q(^{65}\mathrm{Cu}, 3/2^+) = -0.195(4)$ b [14] the absolute value for the quadrupole moment of the ^{68}Cu, 2^+ state is calculated to be $|Q(^{68}\mathrm{Cu}, 2^+, 84.1\,\mathrm{keV})| = 0.110(3)$ b.

To measure the magnetic hyperfine interaction, cobalt and nickel sample hosts were implanted with ^{68m}Cu. Figure 3(b) shows the experimental $R(t)$ function obtained for ^{68m}Cu in a cobalt foil. Three different fractions (f) of Cu nuclei interacting with different local environments have been identified ($f_1 = 22(1)\%$, $f_2 = 32(1)\%$ and $f_3 = 46(2)\%$). Even though the present measurements were performed without an external applied field, the $R(t)$ function is not typical for a random distribution of fields in the foil, as expected for a polycrystalline-like sample. Instead, the $R(t)$ function revealed a preferred orientation of the magnetization along the foil surface, within the detector plane, around 45 degrees in-between detectors. This is presumably due to the rolling process during manufacture and shape anisotropy of the foil.

The analysis of the $f_3 = 46(2)\%$ fraction, resulting in the slowly decaying component of the spectrum, is not compatible with the hyperfine fields expected for Cu in the cobalt host. Apparently, a fraction of the nuclei was implanted into the aluminium sample holder, due to a non-optimal beam focusing. The $f_2 = 32(1)\%$ fraction is assigned to ^{68}Cu interacting with non-identified point defects created during room temperature implantation in the Co foil. The remaining $f_1 = 22(1)\%$ fraction of atoms on unperturbed lattice sites of the Co hcp lattice interact with a strong magnetic field, producing a very clear spectrum from which one obtains the magnetic precession frequency $\omega_L = 1079.1(34)$ Mrad/s.

As reference, one has the precise magnetic frequencies values from previous nuclear magnetic resonance (NMR) measurements for ^{63}Cu in Co, $\omega_L = 1117.8(3)$ Mrad/s, and for ^{65}Cu in Co, $\omega_L = 1198.2(3)$ Mrad/s [26]. Since the magnetic hyperfine field is independent of the Cu isotope embedded in Co, by using the g factor for ^{63}Cu and ^{65}Cu ($g = 1.480(0)$, $g = 1.580(5)$) [27], and eq. (4), one computes $g = g_i\omega_L/\omega_{Li}$, where ω_L is the value obtained in this work for the 2^+, 84.1 keV of ^{68}Cu, and the index i refers to each ^{63}Cu or ^{65}Cu parameters. Two slightly different values for the g factor of the ^{68}Cu, 2^+ state are obtained, which were averaged leading to $|g(2^+, 84.1\,\mathrm{keV})| = 1.429(6)$. Note that the magnetic frequencies ω_L mentioned above from ref. [26] were obtained by nuclear magnetic resonance (NMR) measurements at a temperature of 282 K. The small difference in temperature between the NMR (282 K) and the current TDPAC measurements (295 K) is irrelevant, since the expected hyperfine field changes in Co are smaller than 0.2%. Finally, the absolute value for the magnetic dipole moment of the ^{68}Cu, 2^+ state is determined to be $|\mu(2^+, 84.1\,\mathrm{keV})| = 2.859(13)\,\mu_\mathrm{N}$.

Figure 3(c) shows complementary TDPAC measurements obtained for ^{68m}Cu implanted in a nickel foil. A similar spectrum analysis to the Co case was made,

Table 1: Experimental parameters obtained from fitting the $R(t)$ function. Only relevant parameters for the calculation of the nuclear moments are shown.

	A_{22}^{eff}	f_1 (%)	ω_0 (Mrad/s)	ω_L (Mrad/s)
Cu_2O	−0.13(1)	89	21.3(4)	–
Co	−0.13(1)	22	–	1079.1(34)
Ni	−0.13(1)	44	–	273.7(48)

Table 2: Nuclear moments of the ^{68}Cu(2^+, 84.1 keV) state calculated with the experimental data obtained in this work. Previously measured and extrapolated hyperfine fields as explained in the text have been used.

	$\lvert Q\rvert$ (b)	$\lvert g\rvert$	$\lvert\mu\ (\mu_N)\rvert$
Cu_2O	0.110(3)	–	–
Co	–	1.429(6)	2.859(13)
Ni	–	1.402(43)	2.804(85)
	0.110(3)	1.429(6)	2.857(6)

Table 3: Experimental, additivity extrapolated and shell model g factors and quadrupole moments.

		Experiment[a]		Additivity		Shell model[b]	
	I	g	Q (b)	g	Q (b)	g	Q (b)
^{69}Cu	$3/2^-$	1.8922(7)	−0.147(16)			1.854	−0.1547
^{67}Cu	$3/2^-$	1.6761(4)	−0.174(8)			1.784	−0.1875
^{68}Cu	1^+	2.3933(6)	−0.082(13)	1.930	−0.080(3)	2.367	−0.0945
						2.057[c]	−0.084[c]
	2^+	**(+)1.429(6)**	**(−)0.110(3)**	1.639	−0.160(6)	1.173	−0.190
						1.581[c]	−0.168[c]
	6^-	0.1925(1)	−0.44(2)	0.380		0.254	−0.358
						0.241[c]	−0.474[c]
^{67}Ni	$1/2^-$	1.202(5)				0.874	
	$9/2^+$	−0.125(6)				−0.283	−0.250

[a] Present work (bold) and refs. [14,28].

[b] $\pi\nu pf_{5/2}g_{9/2}$ model space with jj44b interaction; $e^\pi = 1.5\ e$, $e^\nu = 1.1\ e$ and $g_s^\nu = 0.7\ g_s^{free}$ [29].

[c] Inferred from ^{67,69}Cu , ^{67}Ni shell model by additivity.

reveiling that the $R(t)$ function can be described by only two fractions of Cu nuclei in different environments. Again, a slow frequency component is present, $f_2 = 56(3)\%$ of Cu atoms which have landed in the aluminium sample holder. Nonetheless, $f_1 = 44(2)\%$ of the Cu nuclei interact with a well-defined magnetic field, characterized by a magnetic precession frequency $\omega_L = 273.7(48)\,\mathrm{Mrad/s}$.

As reference, one has the magnetic hyperfine field obtained in [30] $B_{hf} = -4.7(1)\,\mathrm{T}$ at 4 K. This value was then rescaled to 105 K using the magnetization saturation curve of [31], obtaining $B_{hf} = -4.6(1)\,\mathrm{T}$. A final extrapolation of the hyperfine magnetic field was performed to 304 K using the time differential perturbed angular distribution (TDPAD) measurements for ^{62}Cu in Ni [32]. From that work the magnetic frequencies, at 105 K and 304 K, were graphically extracted, $\omega_L = 153.8(17)\,\mathrm{Mrad/s}$ and $\omega_L = 135.5(10)\,\mathrm{Mrad/s}$, respectively. One calculates the final extrapolated field $B_{hf} = -4.08(10)\,\mathrm{T}$. With the present experimental frequency, $\omega_L = 273.7(48)\,\mathrm{Mrad/s}$ one obtains $|g(2^+, 84.1\,\mathrm{keV})| = 1.402(43)$. The magnetic dipole moment is determined as $|\mu(2^+, 84.1\,\mathrm{keV})| = 2.804(85)\,\mu_\mathrm{N}$.

From the two independent crosscheck experiments using cobalt ($\mu = 2.859(13)\,\mu_\mathrm{N}$) and nickel ($\mu = 2.804(85)\,\mu_\mathrm{N}$) hosts, the average (error weighted) value of $\mu = 2.857(6)\,\mu_\mathrm{N}$ has been adopted. Tables 1 and 2 summarize the relevant experimental parameters obtained in the present work and the calculated nuclear quadrupole and magnetic moments.

Discussion. – When preparing the present experiment, we had to estimate the nuclear properties of the ^{68}Cu, 2^+ state. Since the structure of the low-lying 1^+, 2^+ doublet is expected to be essentially $(^{68}\mathrm{Cu}; 1^+, 2^+) = (^{69}\mathrm{Cu}; 3/2^-) \times (^{67}\mathrm{Ni}; 1/2^-)$, largely independent of the assumption of a specific configuration, predictions of the nuclear moments may be calculated from experimental values in neighboring nuclei. This empirical approach is expected to include the major part of correlations of the true wave function, even if $Z = 28$, $N = 40$ is not a robust shell closure. The additivity rule for nuclear moments, see, *e.g.*, [33], yields for the quadrupole moments in the stretched $I^\pi = 2^+$ state $Q(^{68}\mathrm{Cu}; 2^+) = Q(^{67,69}\mathrm{Cu}; 3/2^-)$ as $Q(^{67}\mathrm{Ni}; 1/2^-) \equiv 0$, whereas angular momentum re-coupling yields $Q(^{68}\mathrm{Cu}; 1^+) = 1/2 \times Q(^{67,69}\mathrm{Cu}; 3/2^-)$. Similarly, one gets $\mu(^{68}\mathrm{Cu}; 2^+) = \mu(^{67,69}\mathrm{Cu}; 3/2^-) + \mu(^{67}\mathrm{Ni}; 1/2^-)$ and $\mu(^{68}\mathrm{Cu}; 1^+) = 5/6 \times \mu(^{67,69}\mathrm{Cu}; 3/2^-) - 1/2 \times \mu(^{67}\mathrm{Ni}; 1/2^-)$. The validity of additivity of nuclear moments in the vicinity of ^{68}Ni has been discussed by Vingerhoets *et al.* in the framework of shell model calculations [14]. In table 3 experimental data are compared to results inferred from additivity. The data for ^{67}Ni neighbours are listed for comparison. For empirical interpolation the mean value of ^{67,69}Cu values was always used. For g factor and Q of ^{68}Cu, 2^+ positive, respectively negative signs were adopted following the shell model expectation.

When it was noted that the nuclear moments measured in this work were only qualitatively reproduced by the additivity treatment, shell model calculations in the $\pi\nu(f_{5/2}, p, g_{9/2})$ model space above an inert ^{56}Ni core were performed with the jj44b [34] interaction. The results for the copper isotopes and ^{67}Ni are shown in table 3. Even though the moments of the ^{68}Cu, 1^+ ground state are quite well reproduced, the theoretical results for the 2^+ and 6^- state, as well as for ^{67}Ni, are quite far from the experimental ones. For the magnetic moments this is mainly due to the ^{67}Ni, $1/2^-$ value, which is underestimated in the shell model with the effective operator used as specified in the footnotes to table 3.

The deviation in the empirical value, however, points to a more complicated structure beyond the simple $\pi p_{3/2} \times \nu p_{1/2}^{-1}$ configuration of the wave function, which is also observed for the ^{68}Cu, 6^- state. This is even more apparent

in the 2^+ state. Note that shell model interactions fail to predict the correct 1^+-2^+ sequence [14]. Inspection of the shell model wave function indicates a substantial difference in the two wave functions yielding a $\geq 20\% \pi p_{3/2} \times \nu f_{5/2}^{-1}$ component in the 2^+, while it is $< 1\%$ in the 1^+ state, in agreement with ^{67}Ni, $1/2^-$.

This also manifests itself in the observation, that the actual shell model value for the g factor of the 1^+ state is smaller than the one calculated assuming additivity of the shell model values of the ^{67,69}Cu and ^{67}Ni neighbors (also included for comparison in table 3), while for the 2^+ state the opposite is found. It is interesting to note, that the additivity values for the g factors of the 1^+ and 2^+ states, when corrected for this wave function effect, come much closer to the experimental results. Thus it may be concluded, that a successful theoretical shell model description would have to include also particle-hole excitations across the $Z = 28$ shell, in agreement with the observation in [33] for the heavy odd-A copper isotopes. Unfortunately, such calculations are not available for the odd-odd isotopes, and are beyond the scope of the present work. The fact that the ratio of the experimental quadrupole moments of the 2^+ to the one of the 1^+ state is far from the value of about 2, expected both in additivity and the straight shell model, could be a particularly critical check of such calculations, since they would also include the changes of collective properties from one isotope to the next [35].

Conclusions. – The TDPAC technique was used to measure for the first time the electric quadrupole and the magnetic dipole moments of the first excited state in ^{68}Cu$(2^+, 84.1\,\text{keV})$. Values of $Q = -0.110(3)\,\text{b}$ and $\mu = 2.857(6)\,\mu_\text{N}$ were obtained.

The differences between measured and shell model predicted values for the nuclear moments can be explained by limitations of the model space, which excluded proton particle-hole excitations across the $Z = 28$ closed shell. The additivity rules for magnetic and quadrupole moments yield only qualitative estimates for configurations composed of single particle/hole states. This may be traced back to the weak $N = 40$ subshell closure at $Z = 28$.

The present work clearly demonstrates the feasibility of using the ^{68m}Cu/^{68}Cu isomeric decay as a unique copper probe for hyperfine interactions studies in areas such as condensed and soft matter physics, biophysics and chemistry.

* * *

The authors would like to thank the ISOLDE operation and technical teams. We kindly acknowledge Prof. Daniel Galaviz for the valuable suggestions improving the readability of the paper. This project has received funding through the European Union's Seventh Framework Programme for Research and Technological Development under Grant Agreements 262010 (ENSAR) and 289191 (LA3NET), by the Found for Scientific Research-Flanders (G.0983.15) and the KU Leuven BOF (CREA/14/013 and STRT/14/002) from Belgium, by project from the Foundation for Science and Technology (FCT) of Portugal (CERN-FIS-NUC-0004-2015) and by project CICECO-Aveiro Institute of Materials, (POCI-01-0145-FEDER-007679) - FCT Ref. (UID/CTM/50011/2013), financed by national funds through the FCT/MEC and when appropriate co-financed by FEDER under the PT2020 Partnership Agreement. ASF acknowledges the PhD grants support by FCT (SFRH/BD/84743/2012) and KU Leuven. BAB acknowledges NSF grant (PHY-1404442). SP acknowledges the Greek State Scholarships Foundation (I.K.Y.), Project scholarships I.K.Y. from resources of "Education and Lifelong Learning", the European Social Fund (ESF) NSRF, 2007–2013.

REFERENCES

[1] da Silva J. F. and Williams R., *The Biological Chemistry of the Elements*, 2nd edition (Oxford University Press, Oxford) 2002.
[2] Tapiero H., Townsend D. and Tew K., *Biomed. Pharmacother.*, **57** (2003) 386.
[3] Linder M., *Biochemistry of Copper*, 2nd edition (Plenum Press, New York) 1991.
[4] Ambundo E. A., Yu Q., Ochrymowycz L. A. and Rorabacher D. B., *Inorg. Chem.*, **42** (2003) 5267.
[5] Imai S., Fujisawa K., Kobayashi T., Shirasawa N., Fujii H., Yoshimura T., Kitajima N. and Moro-oka Y., *Inorg. Chem.*, **37** (1998) 3066.
[6] Lipton A. S., Heck R. W., de Jong W. A., Gao A. R., Wu X., Roehrich A., Harbison G. S. and Ellis P. D., *J. Am. Chem. Soc.*, **131** (2009) 13992.
[7] Irangu J. K. and Jordan R. B., *Inorg. Chem.*, **42** (2003) 3934.
[8] Butz T., Saibene S., Fraenzke T. and Weber M., *Nucl. Instrum. Methods Phys. Res. A*, **284** (1989) 417.
[9] Butz T., *Hyperfine Interact.*, **52** (1989) 189.
[10] Haas H. and Shirley D. A., *J. Chem. Phys.*, **58** (1973) 3339.
[11] Schatz G. and Weidinger A., *Nuclear Condensed Matter Physics: Nuclear Methods and Applications* (Wiley) 1995.
[12] `http://test-isolde-yields.web.cern.ch`.
[13] Stora T., *Nucl. Instrum. Methods Phys. Res. B*, **317** (2013) 402.
[14] Vingerhoets P., Flanagan K. T., Avgoulea M., Billowes J., Bissell M. L., Blaum K., Brown B. A., Cheal B., de Rydt M., Forest D. H., Geppert C., Honma M., Kowalska M., Krämer J., Krieger A., Mané E., Neugart R., Neyens G., Nörtershäuser W., Otsuka T., Schug M., Stroke H. H., Tungate G. and Yordanov D. T., *Phys. Rev. C*, **82** (2010) 064311.
[15] Mishin V., Fedoseyev V., Kluge H.-J., Letokhov V., Ravn H., Scheerer F., Shirakabe Y., Sundell S. and Tengblad O., *Nucl. Instrum. Methods Phys. Res. B*, **73** (1993) 550.

[16] Köster U., Catherall R., Fedoseyev V. N., Franchoo S., Georg U., Huyse M., Kruglov K., Lettry J., Mishin V. I., Oinonen M., Ravn H., Seliverstov M. D., Simon H., van Duppen P., van Roosbroeck J. and Weissman L., *Hyperfine Interact.*, **127** (2000) 417.
[17] Stachura M., Gottberg A., Johnston K., Bissell M., Garcia Ruiz R., Martins Correia J., Granadeiro Costa A. R., Dehn M., Deicher M., Fenta A. S., Hemmingsen L., Molholt T. E., Munch M., Neyens G., Pallada S., Silva M. R. and Zakoucky D., *Nucl. Instrum. Methods Phys. Res. B*, **376** (2016) 369.
[18] Jäger M., Iwig K. and Butz T., *Hyperfine Interact.*, **198** (2010) 167.
[19] Jäger M., Iwig K. and Butz T., *Rev. Sci. Instrum.*, **82** (2011) 065105.
[20] Jäger M. and Butz T., *Nucl. Instrum. Methods Phys. Res. A*, **674** (2012) 24.
[21] Nagl M. A., Barbosa M. B., Vetter U., Correia J. G. and Hofsass H. C., *Nucl. Instrum. Methods Phys. Res. A*, **726** (2013) 17.
[22] Krane K. S. and Steffen R. M., *Phys. Rev. C*, **2** (1970) 724.
[23] Barradas N. P., Rots M., Melo A. A. and Soares J. C., *Phys. Rev. B*, **47** (1993) 8763.
[24] Lopes A., *Local Probe Studies on Lattice Distortions and Electronic Correlations in CMR Manganites* (Aveiro University) 2006.
[25] de Wijn H. W. and de Wildt J. L., *Phys. Rev.*, **150** (1966) 200.
[26] Kushida T., Silver A. H., Koi Y. and Tsujimura A., *J. Appl. Phys.*, **33** (1962) 1079.
[27] Lutz O., Oehler H. and Kroneck P., *Z. Phys. A*, **288** (1978) 17.
[28] `http://www.nndc.bnl.gov/endsdf/`.
[29] Lisetskiy A. F., Brown B. A., Horoi M. and Grawe H., *Phys. Rev. C*, **70** (2004) 044314.
[30] Kontani M., Asayama K. and Itoh J., *J. Phys. Soc. Jpn.*, **20** (1965) 1737.
[31] Kittel C., *Introduction to Solid State Physics*, 6th edition (John Wiley & Sons, Inc., New York) 1986.
[32] Bleck J., Butt R., Lindenberger K. H., Ribbe W. and Zeitz W., *Z. Phys.*, **263** (1973) 169.
[33] Neyens G., *Rep. Prog. Phys.*, **66** (2003) 633.
[34] Verney D., Ibrahim F., Bourgeois C., Essabaa S., Galès S., Gaudefroy L., Guillemaud-Mueller D., Hammache F., Lau C., Blanc F., Mueller A. C., Perru O., Pougheon F., Roussière B., Sauvage J. and Sorlin O., *Phys. Rev. C*, **76** (2007) 054312.
[35] Sieja K. and Nowacki F., *Phys. Rev. C*, **81** (2010) 061303.